IJARST

International Journal of Advanced Research in Science and Technology

https://doi.org/10.62226/ijarst20241394

ISSN 2319 – 1783 (Print)
ISSN 2320 – 1126 (Online)

Petrography and Geochemistry Study of the Madharam Lamprophyre Dyke, Western Margin of the Proterozoic Pakhal Basin Within Eastern Dharwar Craton, Khammam, Telangana, India

Debapriya Adhikary[1*], Chinchu S.V[1] and Sambuddha Mukherjee[2] and Rajesh Kumar Sahoo[3]

[1] Geological Survey of India, NCEGR, Faridabad-121001 India,[2]Geological Survey of India, Eastern Region, Kolkata-700091, India, [3]Geological Survey of India, Western Region, Jaipur-302004, India

[1]debapriya.adhikary@gmail.com*

ARTICLEINFO

Article history:

Received	01 June 2024
Accepted	10 June 2024
Available online	10 June 2024

Keywords:
Madharam lamprophyre,
Alkaline Lamprophyre,
Khammam Lamprophyre

ABSTRACT

Various lamprophyre types are prevalent throughout the Cuddapah Igneous Province (CIP) and Prakasam Alkaline Province (PAP) in the Eastern Dharwar Craton (EDC), located in southern India. This study focuses on a newly identified lamprophyre dyke situated near the Madharam area in Khammam District, Telangana, India (coordinates 80°15′:17°32′) on the northeastern edge of the EDC. The paper provides an in-depth analysis of the petrography and geochemistry of this lamprophyre. The study area predominantly comprises granitoids from the Peninsular Gneissic Complex (PGC) within the EDC. Geographically, it is flanked by the Proterozoic sedimentary basins of Pakhal to the east and Cuddapah to the south. The Madharam lamprophyre exhibits a characteristic porphyritic-panidiomorphic texture, with clinopyroxene phenocrysts occurring alongside feldspar in the groundmass. Amphiboles present in the rock are of calcic variety (mainly actinolite group). Clinopyroxene is found to be diopside in nature (Wo48-50 En40-41 Fs9-10) and the feldspars show albitic (Or_0Ab85-92 An 6-14) nature. Lower TiO_2 content in the amphibole and clinopyroxene suggests the nature of the lamprophyre is calc-alkaline. The geochemical signatures, such as variable Ba/La ratios and low Nb/La values, suggest minimal to no crustal contamination in the lamprophyre magma. These findings are significant for understanding the evolution of the EDC and provide important constraints on the geodynamics of southern peninsular India.

Introduction:

In India, lamprophyre occurrences span ages from the Precambrian to the Cretaceous period, with the EDC hosting the largest number and variety. Within the EDC, lamprophyres are found in two broad regions: (i) along the western margin of the Cuddapah Basin, primarily in the Wajrakarur Kimberlite Field (WKF), where calc-alkaline and/or shoshonitic lamprophyres have been documented (Pandey et al., 2017a, 2017b, 2018), and (ii) the Prakasam Alkaline Province (PAP) (Leelanandam, 1989) or the 'Cuddapah intrusive province' (Madhavan et al. 1998) To the east of the Cuddapah Basin, at the intersection of the EDC and the Eastern Ghats Mobile Belt (EGMB), the lamprophyres are predominantly of the alkaline variety, with some exhibiting shoshonitic characteristics (Madhavan et al., 1998; Chalapathi Rao, 2004 & 2008).

The lamprophyres of EDC are known to be associated with greenstone belts, granite gneisses and in particular with Kimberlite Clan of Rocks (KCR). Lamprophyres in EDC are reported from WKF, Precambrian Penakacherla Schist Belt, Mudigubba lamprophyre at the western margin of Cuddapah basin, Bayyaram Lamprophyre at the northeastern margin of the EDC at the western margin of Pakhal basin, Khammam district and lamprophyres of PAP. Some of the lamprophyres are reported in NE margin of EDC to the north of Khammam at Polayapalli. In Nallamalai fold belt of Cuddapah basin, earlier K. Appavadhanulu (1971) followed by NMS Rock (1991) classified mafic intrusive as lamprophyres but, Scott Smith confirmed these rocks as lamproites. Dominantly two generations of lamprophyres are found in EDC viz. Neo-Archaean age and Meso-Proterozoic ages. Archaean lamprophyres are linked with calc-alkaline granitoids and coeval mafic-ultramafic rocks. The primary country rock in the study area is granitoid. To the east lies the Proterozoic Pakhal Basin, and to the south, the Proterozoic Cuddapah Basin. The lamprophyre under investigation is intruded within the granitoids of the EDC.

Regional Geology:

In the Khammam district few isolated lamprophyre are reported which is intruded within the granite body

(Appavadhanulu 1971; Subrahmanyam et al. 1987; Meshram et al. 2015, Adhikary et al 2022, Adhikary et al. 2024a and 2024b) (Fig:1). Lamprophyric magma are formed during low degree of partial melting of upper mantle at approx depth of 100-150 km (Rock 1991 and Mitchell R H 1995).Normally this kind of magmas contain high amount of volatiles (F,CO_2,H_2O) and REE (Ulrych et al.1993). This paper presents a detailed petrographic and geochemical analysis of the lamprophyre. The dyke, which is approximately 1 to 2 meters wide with an exposed strike length of about 30 meters, trends N35°W. These dykes have a sharp contact with the host granitoids and display a branching nature (Fig:2A & 2B). However, along the margin of the dyke no chilied margin effect is observed. Dykes also cut across the foliation of the granitoids, it also indicates the intrusive relationship between host rock and the lamprophyre. Megascopically, this lamprophyre dykes are mesocratic to melanocratic, fine grained in nature. Phenocrysts are present in the dykes and also uniformly distributed within matrix. Clinopyroxene, amphibole and biotite are present as phenocrysts within the melanocratic matrix component.

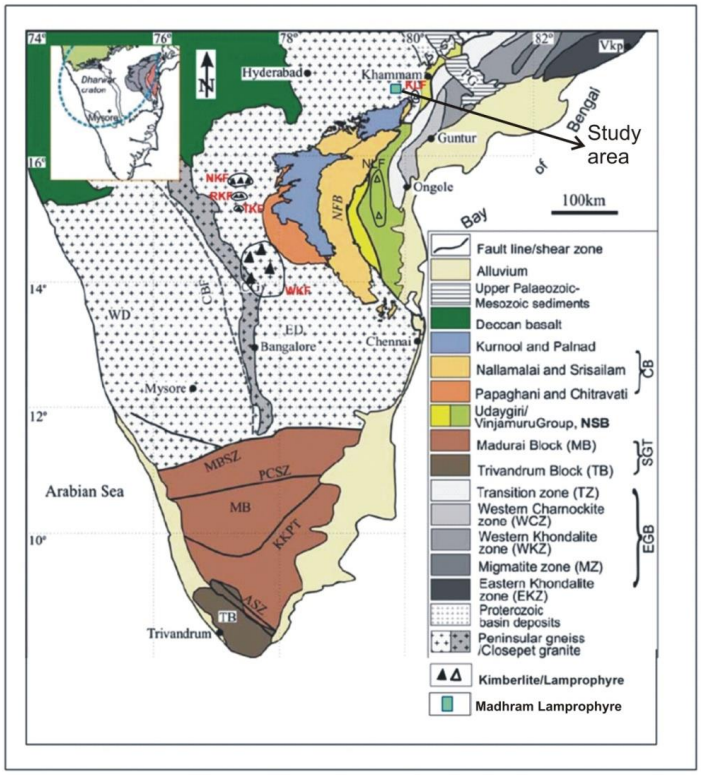

Fig.1. Location of study area in Khammam district, Telangana (after Naqvi, 2005).

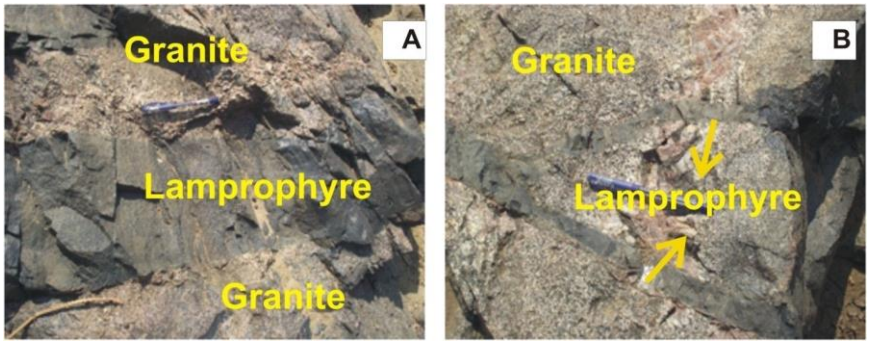

Fig: 2A Lamprophyre at Madharam area show sharp contact with basement granitoids.
Fig:2B Lamprophyre at Madharam area show branching nature.

Analytical techniques:

The mineral chemistry of various phases in the Madharam lamprophyre was analyzed using a CAMECA SX100 Electron Probe Micro Analyzer (EPMA) at GSI facilities in Kolkata and Faridabad. The analysis utilized an acceleration voltage of 15 kV, a beam current of 20 nA, a beam diameter of 1 µm, and a counting time of 10 seconds. The microprobe was calibrated with albite for Na and Al, rhodonite for Mn, diopside for Ca and Mg, TiO for Ti, orthoclase for K and Si, chromium for Cr, and almandine for Fe. The results of selected and representative mineral phase analyses are presented in Tables 1, 2, and 3.

Whole rock major and trace element analyses were conducted at the Geological Survey of India's Chemical Laboratory in Kolkata. Major oxides were analyzed using

X-ray fluorescence spectrometry, while trace and rare earth element (REE) concentrations were determined using ICP-MS. The precision for all analyzed elements is better than 2% at 100 times the detection limit. Several standards were analyzed alongside the samples to ensure accuracy and precision. Table: presented the data of major oxide, trace elements and REE. Standardized CIPW norms for all samples were automatically computed using the IgROCS computer program (Verma et al.2013).

Petrography and mineral chemistry:

Petrographic studies show that Madharam lamprophyre sample consists of clinopyroxene, amphibole,biotite, feldspar and apatite. In this rock amphibole is present as a phenocryst and the groundmass is made up of feldspar and Cpx. amphibole crystal are medium to large in size (FIG:3A,B,C&D). Overall the rock shows porphyritic-panidiomorphic texture. Euhedral shaped amphiboles make up glomeroporphyritic texture. Clinopyroxene occursas microphenocryst within the groundmass. Within the amphibole phenocrysts, apatite inclusion is present. Carbonate also present in the rock, which is replaced olivine and clinopyroxene phenocryst. Modal analysis shows that this lamprophyre contains equal amount of clinopyroxene and amphibole.

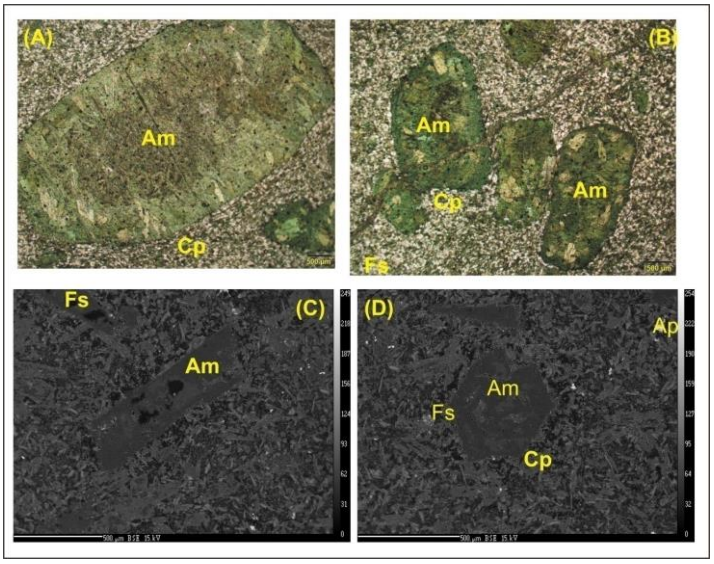

Fig:3. Photomicrographs of the Madharam lamprophyre: (A and B) Clusters of well-formed amphibole phenocrysts displaying a panidiomorphic-glomerophyric texture (observed under plane-polarized light); (C) Large amphibole phenocrysts and a clinopyroxene groundmass [Backscattered electron (BSE) image]. (D)Hexagonal amphibole crystal along with Cpx and feldspar [BSE image].

The chemical composition of different mineral phases is outlined as follows:

Clinopyroxene:

In the lamprophyre sample being analyzed, the clinopyroxenes are predominantly diopsidic (Wo48-50 En40-41 Fs9-10) (see Fig. 4A). When aluminum (Al) and titanium (Ti) values for clinopyroxene are plotted on a Ca (a.p.f.u) versus Ti (a.p.f.u) diagram (refer to Fig. 4C), they indicate an orogenic origin of the lamprophyre.

Amphibole:

Predominantly, the amphiboles in this lamprophyre are of the actinolite variety (see Fig. 4B). Actinolite is typically absent in igneous rocks, suggesting its formation through metamorphism involving hydrous melts and existing amphiboles. (Leake et. al 1997) The lamprophyre samples show depletion in Al2O3, K2O, and TiO2, indicating a calc-alkaline magma nature. This is evidenced by a TiO2 (wt%) versus SiO2 (wt%) plot (after Rock, 1991) (Fig:4D) indicating the calc-alkaline nature of the studied lamprophyres.

Feldspar:

In the Madharam lamprophyre feldspars are present essentially as a groundmass part. The feldspars are of albitic composition. The average composition range of the feldspar is (Or0 Ab85-92 An 6-14). The depletion in FeO and prevalence of alkali feldspar characterize this calc-alkaline lamprophyre as spessartine. (Le Maitre, 2002).

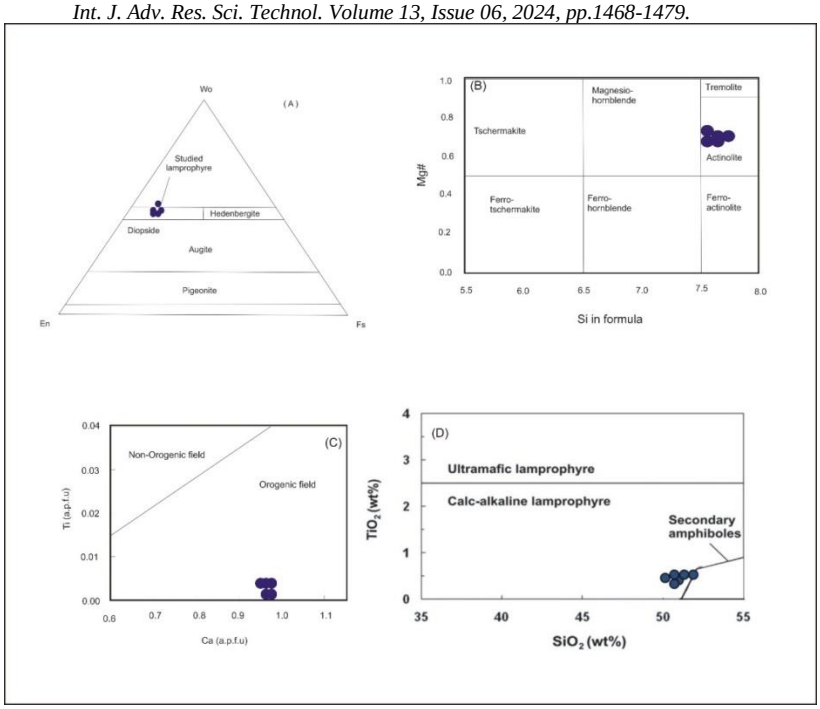

Fig:4. (A) Diagram illustrating the diopsidic nature of clinopyroxenes in the Madharam lamprophyre. (B) Si vs. Mg# plot for amphibole classification (adapted from Leake et al., 1997) in the Madharam lamprophyre. (C) Ti (a.p.f.u) vs. Ca (a.p.f.u) plot (based on Sun and Bertrad, 1991) showing the orogenic characteristics of clinopyroxene. (D) TiO2 (wt%) vs. SiO2 (wt%) plot (according to Rock, 1991) indicating the calc-alkaline nature of the studied Madharam lamprophyre.

Table 1: Representative analyses (wt%) of clinopyroxene from the Madharam lamprophyres (ML)

Oxide Wt%	1	2	3	4	5	6	7	8
	CPX 1	CPX 2	CPX 3	CPX 4	CPX 5	CPX 6	CPX 7	CPX 8
SiO2	53.13	54.1	52.89	53.34	53.21	53.31	53.62	53.83
TiO2	0.22	0.09	0	0.14	0.05	0.04	0.03	0.06
Al2O3	1.6	0.61	0.37	1.1	0.93	0.46	0.65	0.62
Cr2O3	0.18	0.1	0.1	0.06	0.02	0.18	0.06	0
FeO	6.75	6.31	6.03	6.63	7.56	7.85	7.36	7.27
MnO	0.2	0.36	0.26	0.12	0.3	0.48	0.26	0.15
MgO	14.78	15.04	14.16	14.95	13.79	13.73	13.85	14.25
CaO	23.57	24.24	24.41	23.52	24.19	24.1	24.69	24.21
Na2O	0.57	0.39	0.35	0.47	0.5	0.46	0.46	0.49
K2O	0.01	0	0	0	0	0	0.01	0
Total	101.01	101.24	98.57	100.33	100.55	100.61	100.99	100.88
Cations for 6 Oxygen atoms								
Si	1.94	1.97	1.98	1.96	1.96	1.97	1.97	
Ti	0.01	0	0	0	0	0	0	0
Al	0.07	0.03	0.02	0.05	0.04	0.02	0.03	0.03
Cr	0.01	0	0	0	0	0.01	0	0
Fe3+	0.07	0.05	0.04	0.06	0.06	0.06	0.06	0.05
Fe2+	0.13	0.14	0.15	0.15	0.17	0.18	0.17	0.17
Mn	0.01	0.01	0.01	0	0.01	0.02	0.01	0
Mg	0.8	0.82	0.79	0.82	0.76	0.76	0.76	0.78
Ca	0.92	0.95	0.98	0.93	0.96	0.95	0.97	0.95
Na	0.04	0.03	0.03	0.03	0.04	0.03	0.03	0.03
K	0	0	0	0	0	0	0	0
Total	4	4	4	4	4	4	4	4
En	0.43	0.43	0.41	0.43	0.4	0.4	0.4	0.41
Fs	0.07	0.08	0.08	0.08	0.09	0.1	0.09	0.09
Wo	0.5	0.5	0.51	0.49	0.51	0.5	0.51	0.5

Table 2: Representative analyses (wt%) of amphiboles from the Madharam lamprophyres

Oxide Wt%	1	2	3	4	5	6	7	8
	AMP1	AMP2	AMP3	AMP4	AMP5	AMP6	AMP7	AMP8
SiO2	49.44	49.39	46.64	45.31	45.92	46.55	50.11	49.81
TiO2	0.99	0.98	1.12	1.42	1.12	1.03	0.48	0.48
Al2O3	5.96	6.21	7.98	10.72	9.11	8.42	5.81	6.02
Cr2O3	0.18	0.22	0.33	0.17	0.22	0.23	0	0
FeO	11.01	11.07	12.89	11.9	12.03	12.13	11.34	12.21
MnO	0.08	0.08	0.29	0.07	0.29	0.22	0.14	0.17
MgO	15.82	15.74	13.73	13.86	14.13	14.34	15.55	14.95
NiO	0	0.11	0.13	0.01	0	0	0	0
ZnO	0	0	0.08	0.02	0	0	0.24	0
CaO	12.12	12.48	12.29	12.44	12.4	12.32	12.74	12.72
Na2O	0.96	1.12	1.2	1.9	1.53	1.52	0.72	0.82
K2O	0.46	0.33	0.82	0.45	0.49	0.46	0.4	0.49
Total	97.02	97.73	97.50	98.27	97.24	97.22	97.53	97.67
Cations for 23 oxygen atoms								
Si	7.12	7.09	6.83	6.56	6.70	6.79	7.22	
Ti	0.11	0.11	0.12	0.15	0.12	0.11	0.05	0.05
Al	1.01	1.05	1.38	1.83	1.57	1.45	0.99	1.03
Cr	0.02	0.02	0.04	0.02	0.03	0.03	0.00	0.00
Fe3+	0.41	0.31	0.33	0.26	0.35	0.36	0.27	0.20
Fe2+	0.92	1.02	1.24	1.18	1.12	1.12	1.09	1.27
Mn	0.01	0.01	0.04	0.01	0.04	0.03	0.02	0.02
Mg	3.40	3.37	3.00	2.99	3.08	3.12	3.34	3.22
Ca	1.87	1.92	1.93	1.93	1.94	1.93	1.97	1.97
Na	0.27	0.31	0.34	0.53	0.43	0.43	0.20	0.23
K	0.08	0.06	0.15	0.08	0.09	0.09	0.07	0.09
Total	15.22	15.28	15.40	15.54	15.46	15.44	15.21	15.29

Table 3: Selected mineral chemistry data (wt%) of feldspar in the Madharam lamprophyre

Oxide Wt%	1 FELDS1	2 FELDS2	3 FELDS3	4 FELDS4	5 FELDS5	6 FELDS6	7 FELDS7	8 FELDS8
SiO2	68.5	68.69	64.33	69.33	68.33	64.18	68.21	67.5
Al2O3	19.28	19.21	18.07	19.46	19.59	17.59	20.19	20.59
FeO	0.07	0.1	0.11	0.11	0.05	0.7	0	0.05
CaO	0.53	0.4	0	0.49	0.6	0.01	0.83	1.15
Na2O	11.18	11.18	0.3	11.34	10.29	0.23	11.69	10.99
K2O	0.1	0.05	16.1	0.06	0.11	16.1	0.05	0.38
BaO								
Total	99.66	99.63	98.91	100.79	98.97	98.81	100.97	100.66
Cations for 8 Oxygen atoms								
Si	3.00	3.01	3.00	3.00	3.00	3.01	2.96	2.94
Al	1.00	0.99	0.99	0.99	1.01	0.97	1.03	1.06
Ti	0.00	0.00	0.00	0.00	0.00	0.00	0.00	0.00
Fe	0.00	0.00	0.00	0.00	0.00	0.03	0.00	0.00
Ca	0.02	0.02	0.00	0.02	0.03	0.00	0.04	0.05
Na	0.95	0.95	0.03	0.95	0.88	0.02	0.98	0.93
K	0.01	0.00	0.96	0.00	0.01	0.96	0.00	0.02
Ba								
Total	4.98	4.97	4.99	4.98	4.93	4.99	5.02	5.00
Or	0.57	0.29	97.25	0.34	0.68	97.82	0.27	2.10
Ab	96.89	97.78	2.75	97.34	96.22	2.12	95.96	92.54
An	2.54	1.93	0.00	2.32	3.10	0.05	3.77	5.35

Geochemistry:

Major oxides

Variations in geochemical data for major, minor and trace elements are very less for the Madharam lamprophyres (ML) (Table 4, 5 & 6). The feldspar compositions exhibit high MgO (11.22–12.01 wt%) and CaO (12.27–13.12 wt%), with lower Al2O3 (8.84–9.12 wt%), indicating a sub-alkaline nature. There is a positive correlation between MgO, CaO, and Fe2O3, and a negative correlation between MgO, SiO2, Al2O3, and Na2O, suggesting minimal fractionation (see Fig. 5 A to F). Compared to the global average calc-alkaline lamprophyre composition (MgO: 7 wt%; CaO: 7 wt%; Al2O3: 14 wt%; Rock 1991, p.78), the ML are enriched in MgO and CaO. They are classified as calc-alkaline based on classification diagrams (Fig. 6A and B). Post-magmatic alteration minimally affected the geochemical nature of the lamprophyres, as indicated by positive correlations among LILEs and between LILEs and HFSE (Fig. 7A to D). Ti contents in the ML are lower than those in within-plate lamprophyres (Fig. 8A). The ML are predominantly sodic (Na2O/K2O > 2) and fall along the calc-alkaline-shoshonite boundary in the Na2O vs. K2O diagram (Fig. 7B). The TiO2/Al2O3 vs. Zr/Al2O3 plot (Fig. 8C) suggests that the ML were emplaced in a continental-arc or post-collisional arc setting.

Table 4: Representative major oxide analysis of Madharam lamprophyres

Oxide Wt%	PCS/323(1)/DA	PCS/323(2)/DA	PCS/323(3)/DA	PCS/323(4)/DA	PCS/323(5)/DA
SiO2	50.47	50.65	51.25	50.64	51.01
TiO2	0.69	0.72	0.73	0.68	0.72
Al2O3	9.12	8.45	8.97	9.10	9.10
Total Fe as Fe2O3	8.52	7.5	7.9	8.54	8.40
MnO	0.18	0.18	0.19	0.18	0.18
MgO	11.22	12.01	11.65	11.24	11.22
CaO	12.27	13.12	12.9	12.88	12.70
Na2O	2.18	2.09	2.15	2.14	2.10
K2O	1.07	1.12	1.1	1.09	1.12
P2O5	0.92	0.95	0.9	0.98	0.89
LOI	1.52	1.54	1.62	1.6	1.6
Mg#	76.815	80.114	78.769	80.103	78.537
Total	98.16	98.33	99.36	99.07	99.04
Q	0	0	0	0.00	
Or	6.58	6.88	6.69	6.66	6.59
Ab	19.22	18.38	18.73	18.90	18.72
An	12.44	10.77	11.91	11.88	11.87
Di	35.79	40.18	38.24	38.88	38.77
Hy	15.76	12.16	14.3	13.77	14.10
Ol	3.86	5.5	4.01	4.02	4.80
Mt	2.73	2.4	2.5	2.60	2.60
Il	1.36	1.42	1.42	1.39	1.38
Ap	2.22	2.28	2.14	2.23	2.25

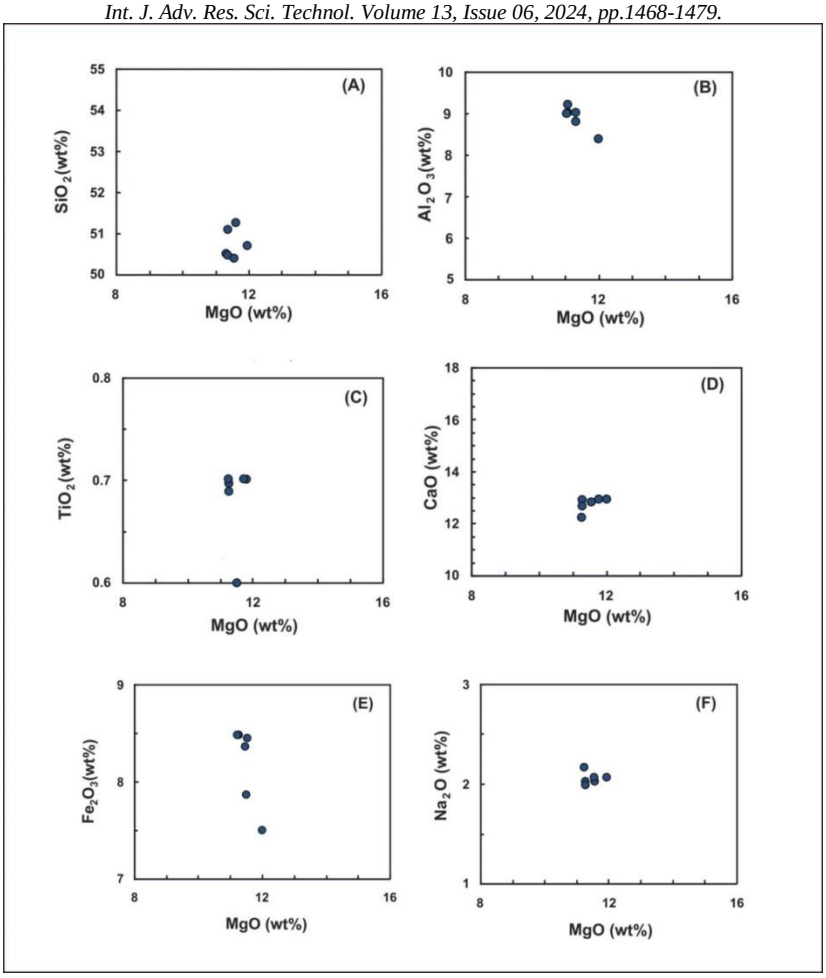

Fig:5. Bivariate plots (A) MgO (wt%) vs. SiO2 (wt%), (B) MgO (wt%) vs. Al2O3 (wt%), (C) MgO (wt%) vs. TiO2 (wt%), (D) MgO (wt%) vs. CaO (wt%), (E) MgO (wt%) vs. Fe2O3 (wt%), and (F) MgO (wt%) vs. Na2O (wt%) for the Madharam lamprophyre demonstrate clear fractionation trends.

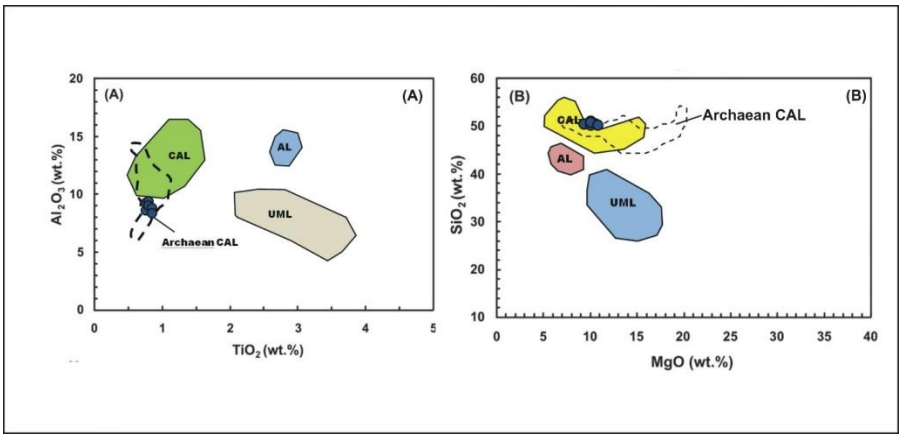

Fig. 6 shows classification plots for the Madharam lamprophyres: (A) Al2O3 (wt%) vs. TiO2 (wt%) and (B) MgO (wt%) vs. SiO2 (wt%). Classification fields including Calc-alkaline lamprophyres (CAL), Alkaline lamprophyres (AL), Ultramafic lamprophyres (UML), and Archaean CAL from various cratons are adapted from Lefebvre et al. (2005).

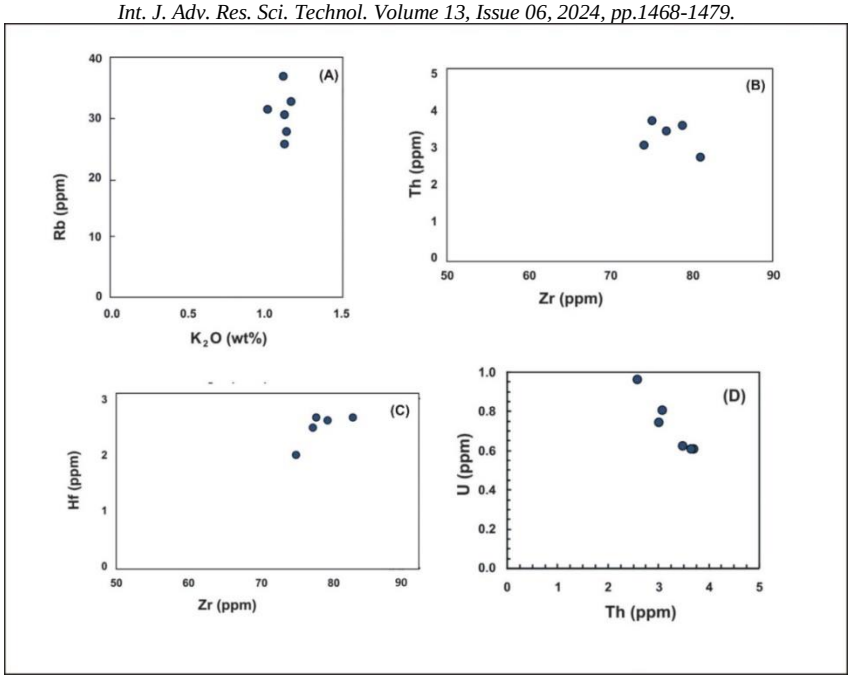

Fig. 7 illustrates plots: (A) K2O (wt%) vs. Rb (ppm), (B) Zr (ppm) vs. Th (ppm), (C) Zr (ppm) vs. Hf (ppm), and (D) Th (ppm) vs. U (ppm), demonstrating positive correlations among LILEs and HFSEs in the Madharam lamprophyre.

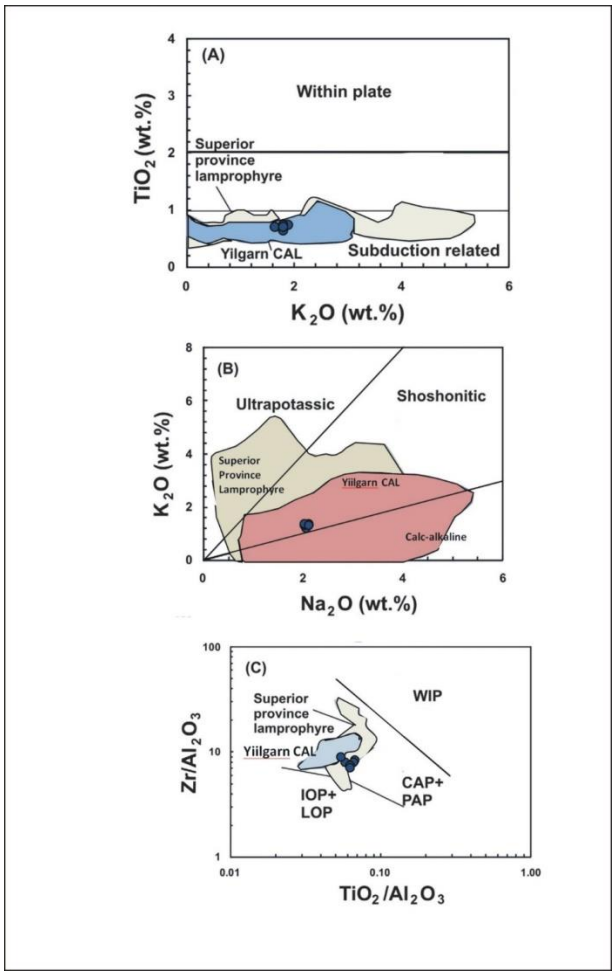

Fig. 8 includes: (A) K2O (wt%) vs. TiO2 (wt%) discrimination plot (adapted from Thorpe, 1987) for distinguishing mafic alkaline rocks related to within-plate and subduction settings, (B) K2O-Na2O bivariate plot (based on Turner et al., 1996) highlighting the sodic and calc-alkaline nature of the ML, and (C) Zr/Al2O3 vs. TiO2/Al2O3 tectonic discrimination diagram (Muller and Groves, 2000) indicating the strong arc affinity of the ML. Data for CAL lamprophyres from the Yilgarn area are sourced from Currie and Williams (1993), and from the Superior Province from Wyman

and Kerrich (1989). Fields: WIP – within-plate; CAP – continental arc; PAP – post-collisional arc; IOP – initial oceanic arc.

Table 5: Representative trace element analysis of Madharam lamprophyre (ppm)

Oxide Wt%	PCS/323(1)/DA	PCS/323(2)/DA	PCS/323(3)/DA	PCS/323(4)/DA	PCS/323(5)/DA
Sc	52	62	55	60.00	58.00
V	148	153	180	177.00	171.00
Cr	461	463	632	460.00	497.00
Co	57	50	62	52.00	55.00
Ni	227	238	247	230.00	232.00
Cu	50	48	55	54.00	51.00
Zn	101	91	110	97.00	99.00
Ga	17	14	15	12.00	16.00
Rb	32	27	36	28.00	31.00
Sr	432	410	478	417.00	402.00
Y	20	26	22	21.00	22.00
Zr	82	76	78	79.00	77.00
Nb	4	3	5	5.00	5.00
Ba	497	522	601	525.00	547.00
Hf	2.7	2.1	2.6	2.50	2.70
Ta	1.24	0.61	0.98	0.77	0.99
Pb	5	5	5	5.00	5.00
Th	2.8	3.1	3.9	3.80	3.60
U	0.9	0.7	0.6	0.60	0.70

Table 6: Representative analysis of REEs in the ML (ppm)

Oxide Wt%	PCS/323(1)/DA	PCS/323(2)/DA	PCS/323(3)/DA	PCS/323(4)/DA	PCS/323(5)/DA
La	25.5	27.2	32.2	31.30	29.50
Ce	45.5	48.3	50.4	47.30	46.50
Pr	8.46	8.58	8.97	8.00	8.22
Nd	40.1	37.6	44.2	41.25	40.45
Sm	9.3	9.5	9.8	9.70	9.60
Eu	2.88	2.28	2.66	3.01	2.89
Gd	7.03	5.60	6.25	6.21	5.75
Tb	1.02	0.78	1.06	1.01	1.00
Dy	4.67	3.62	4.15	4.10	4.50
Ho	0.86	0.61	0.69	0.70	0.73
Er	1.95	1.75	1.9	1.80	1.90
Tm	0.32	0.25	0.27	0.26	0.29
Yb	1.88	1.53	1.9	1.80	1.70
Lu	0.29	0.24	0.26	0.25	0.26

Minor elements:

The trace element analysis of the Madharam lamprophyres indicates moderate enrichment in large-ion-lithophile elements (LILE), with Ba concentrations up to 601 ppm and Sr up to 432 ppm. High values of Mg# (> 76.81), Ni (> 227 ppm), and Cr (> 461 ppm) suggest that these lamprophyres likely originated from moderately fractionated, primary mantle-derived melts (see Rock, 1991). The Th–Hf–Nb/2 discrimination diagram (Fig. 9) designed for lamproitic and lamprophyric rocks (Krmíček et al., 2011; Çoban et al., 2012) suggests that the ML may be of orogenic geodynamic setting. The chondrite-normalized REE pattern reveals enrichment of LREE over HREE (Fig. 10A) with an average LaN/YbN ratio of 15.00 in the ML. The presence of a very high Mg# suggests partial melting phenomena. The primitive-mantle normalized multi-element plot (Fig. 10B) exhibits distinct negative spikes at Nb-Ta, Zr-Hf, and Ti, similar to trends observed in global calc-alkaline lamprophyres. Negative HFSE anomalies suggest calc-alkaline magmas, likely influenced by either slab melting or mantle wedge melting. For that reason this magma is rich in volatile and chemically heterogeneous due to

subduction (Wilson,1989). The elevated LILE/HFSE ratios in this lamprophyre suggest the separation of mobile elements within the descending crustal fragment (Hawkesworth et al., 1994; Thirlwall et al., 1994; Pearce, 2008). The lack of a Eu anomaly in the REE pattern diagram and a negative Sr anomaly in the primitive mantle normalized multi-element diagram indicate that this magma could originate from a depleted mantle. The Th/La ratio serves as an indicator of crustal contamination (Sun and McDonough, 1989). All the geochemistry and petrography study indicate our lamprophyre is probably crustal contamination free and retain the original mantle composition, which is very useful for mantle study.

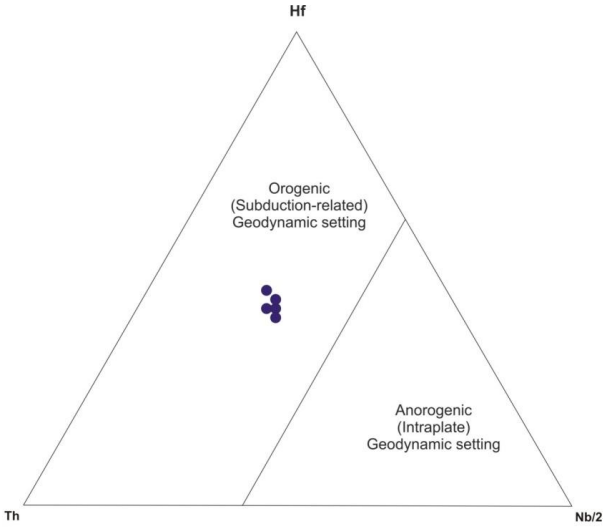

Fig:9. The Hf-Th-Nb/2 ternary tectonic discrimination diagram (adapted from Krmíčˇek et al., 2011) demonstrates the orogenic affinity of the ML samples.

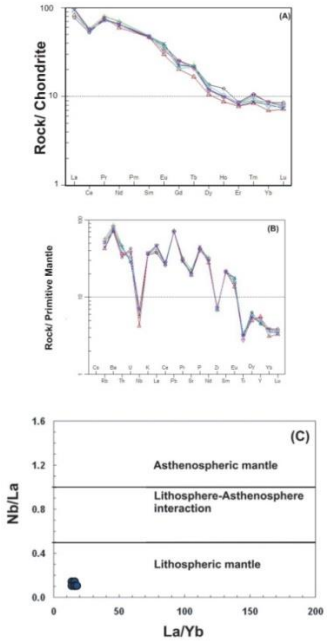

Fig: 10 (A) Chondrite-normalized REE distribution pattern (adapted from Evenssen et al., 1978) and (B) Primitive mantle-normalized multi-element spider diagram (based on Sun and McDonough, 1989) for the ML. (C) Plot of La/Yb versus Nb/La (after Smith et al., 1999), indicating minimal asthenospheric contribution to the mantle source region of the ML.

Discussion:

The Madharam Lamprophyre melt may have originated from a depleted mantle source that had already undergone some degree of partial melting during continental crust formation. This mantle source was affected by later subduction during which LILEs and HFSEs were added to the melt. The geochemical data confirms depletion in TiO2 and Al2O3 content and enrichment in LILEs in the ML. Significant depletion of HFSEs is likely due to the presence of Ti-bearing phases such as rutile/ilmenite in the source mantle melt. The HFSE/LREE ratio provides insights into the mantle source region (Smith et al., 1999) (Fig. 10C). Low Nb/La (<0.2) values suggest the lamprophyre originated from the lithospheric mantle with Nb/La < 0.5, contrasting with OIB-like asthenospheric mantle where

Nb/La > 1. The Ba/Rb ratio, relative to Rb/Sr, confirms the presence of amphibole in the source, indicative of a common subduction-modified mantle wedge (Furman and Graham, 1999). Porphyritic to glomeroporphyritic textures in the rocks indicate crystal fractionation or accumulation driven by amphibole crystallization in the mantle wedge. As previously discussed, the ML exhibit an arc setting based on major oxide diagrams for mafic alkaline lavas and the Zr/Al2O3 vs. TiO2/Al2O3 tectonic discrimination diagram (Fig. 8C) for potassic igneous rocks.

Conclusion:

The ML, located on the edge of the Proterozoic Pakhal Basin, exhibit a porphyritic-panidiomorphic texture characterized by phenocrysts of amphibole, microphenocrysts of clinopyroxene, and a groundmass predominantly composed of feldspar. Mineral chemistry analysis confirms the calc-alkaline nature of these lamprophyres. Anomalies in Nb-Ta, Zr-Hf, and Ti observed in the primitive mantle normalized multi-element plots align closely with global calc-alkaline lamprophyres. Various geochemical ratios (such as Hf/Sm, Ta/La, Th/Yb, Nb/Yb, La/Nb, Ba/Nb) indicate fluid-related subduction metasomatism in the mantle source of the lamprophyre melt. Recently, few lamprophyres have been identified in the western margin of the Pakhal Basin near Bayyaram (Meshram et al 2015),Thirtal (Adhikary,2024 a&b) and now Madharam. This identifying lamprophyre indicates that this may be a new identified lamprophyre magmatism zone with in the EDC.

Acknowledgment:

The authors acknowledge the Director General of the Geological Survey of India for granting permission to publish this manuscript. They also appreciate the support received from various officials during the project, both administratively and technically. Special thanks are extended to Dr. S. Raju, retired DG of GSI & NMH, M-IV, CHQ, Kolkata, for his guidance. The authors are grateful to Dr. Saibal Ghosh, Deputy DG, M-IVC, CHQ & NMH-IV, GSI, Kolkata, for his support and encouragement throughout the project. They also acknowledge Shri. Sanjoy Bharti, Director of NCEGR, Kolkata, for his valuable assistance. The author also express thanks to officers and staffs of Petrology- especially EPMA laboratories of NCEGR Kolkata and Faridabad. Smt.Pushp Lata,Dy.Director General, NCEGR, Faridabad is gratefully acknowledged for her valuable support for preparing this manuscript.

References:

Adhikary, D.; and S.V Chinchu (2024a). Petrology and geochemistry of lamprophyres from Tirthal area, in eastern margin of the Eastern Dharwar Craton, Khammam, Telangana, India. International Journal of Innovative Research in Engineering & Multidisciplinary Physical Sciences, Volume 12, Issue 2 (March-April 2024). Retrieved from https://www.ijirmps.org/research-paper.php?id=230594.

Adhikary, D.; S.V Chinchu; Sahoo, R.K.; and Mukherjee, S. (2024b). Petrography and geochemistry study of the Thirtal lamprophyre dyke left bank of Muneru River, in eastern margin of the Eastern Dharwar Craton, Khammam, Telangana, India. International Journal of Advanced Research in Science and Technology, Volume 13, Issue 05, 2024, pp. 1404-1411. https://doi.org/10.62226/ijarst20241375.

Adhikary, D.; Mukherjee, S.; and Sahoo, R. (2022). Lamprophyre cluster within the granite terrain adjoining the western margin of Proterozoic Pakhal basin, Southern India. Indian Journal of Geosciences, Volume 76, No.1, pp. 1-12.

Appavadhanulu, K. (1971). A short note on the lamprophyre dykes in parts of Khammam district, Andhra Pradesh. Ind. Minerals, 25, 387-398.

Chalapathi Rao, N.V. (2008). Precambrian alkaline potassic-ultrapotassic, mafic-ultramafic magmatism in peninsular India. J. Geol. Soc. India, 72, 57–84.

Chalapathi Rao, N.V.; Gibson, S.A.; Pyle, D.M.; and Dickin, A.P. (2004). Petrogenesis of Proterozoic kimberlites and lamproites from the Cuddapah basin and the Dharwar craton, southern India. J. Petrol., 45, 907–948.

Coban, H.; Karacik, Z.; and Ece, O.I. (2012). Source contamination and tectonomagmatic signals of overlapping Early to Middle Miocene orogenic magmas associated with shallow subduction and asthenospheric mantle flows in Western Anatolia: a record from Simav (Kutahya) region. Lithos, 140–141, 119–141.

Currie, K.L.; and Williams, P.R. (1993). An Archean calc-alkaline lamprophyre suite, northeastern Yilgarn Block, western Australia. Lithos, 31, 33–50.

Evensen, N.M.; Hamilton, P.J.; and O'Nions, R.K. (1978). Rare earth abundances in chondritic meteorites. Geochim. Cosmochim. Acta, 42, 1199–1212.

Furman, T.; and Graham, D. (1999). Erosion of lithospheric mantle beneath the East African Rift system: geochemical evidence from the Kivu volcanic province. Lithos, 48, 237–262.

Hawkesworth, C.J.; Gallagher, K.; Hergt, J.M.; and McDermott, F. (1994). Destructive plate margin magmatism: Geochemistry and melt generation. Lithos, 33, 169–188.

Krmíček, L.; Cempírek, J.; Havlín, A.; Přichystal, A.; Houzar, S.; Krmíčková, M.; and Gadas, P. (2011). Mineralogy and petrogenesis of a Ba–Ti–Zr-rich peralkaline dyke from Šebkovice (Czech Republic): recognition of the most lamproitic Variscan intrusion. Lithos, 121, 74–86.

Leelanandam, C. (1989). The Prakasam Alkaline Province in Andhra Pradesh, India. Journal of Geological Society of India, 34, 25-45.

Leake, B.E., et al. (1997). Nomenclature of amphiboles: report of the subcommittee on amphiboles of the

international mineralogical association, commission on new minerals and mineral names. Am. Mineral., 82, 1019–1037.

Lefebvre, N.; Kopylova, M.; and Kivi, K. (2005). Archaean calc-alkaline lamprophyres of Wawa, Ontario, Canada: unconventional diamondiferous volcaniclastic rocks. Precambrian Res., 138, 57–87.

Le Maitre, R.W. (Ed.) (2002). Igneous Rocks: A Classification and Glossary of Terms. Recommendations of the International Union of Geological Sciences Subcommission on the Systematics of Igneous Rocks. Cambridge University Press, Cambridge, 236pp.

Madhavan, V.; David, K.; Mallikharjuna Rao, J.; Chalapathi Rao, N.V.; and Srinivas, M. (1998). Comparative study of lamprophyres from the Cuddapah Intrusive Province (CIP) of Andhra Pradesh, India. J. Geol. Soc. India, 52, 624–642.

Meshram, T.M.; Shukla, D.; and Behera, K.K. (2015). Alkaline lamprophyre (camptonite) from Bayyaram area, NE margin of the Eastern Dharwar Craton, southern India. Curr. Sci., 109, 1931–1934.

Mitchell, R.H. (1995). Kimberlites, orangeites and related rocks. Plenum Press, New York, 410p.

Muller, D.; and Groves, D.I. (2000). Potassic Igneous Rocks and Associated Gold-Copper Mineralization. Springer, Berlin, p. 252.

Naqvi, S.M. (2005). Geology and Evolution of the Indian Plate (From Hadean to Holocene – 4 Ga to 4 Ka). Capital Publishing Company, New Delhi, 450p.

Pandey, A.; Chalapathi Rao, N.V.; Ramananda Chakrabarti; Praveer Pankaj; Dinesh Pandita; Rohit Pandey; and Samarendra Sahoo (2018). Post-collisional calc-alkaline lamprophyres from the Kadiri greenstone belt: Evidence for the Neoarchean convergence-related evolution of the Eastern Dharwar Craton and its schist belts. Lithos, 320–321, 105–117.

Pandey, A.; Pandey, R.; Pandit, D.; Pankaj, P.; Chalapathi Rao, N.V. (2017b). A note on the origin of Clinopyroxene megacrysts from the Udiripikonda lamprophyre, Eastern Dharwar craton, southern India. J. Indian Geophys. Union, 21, 124–131.

Pandey, A.; Chalapathi Rao, N.V.; Pandit, D.; Pankaj, P.; Pandey, R.; Sahoo, S.; and Kumar, A. (2017a). Subduction-Tectonics in the evolution of the eastern Dharwar craton, southern India: Insights from the post-collisional calc-alkaline lamprophyres at the western margin of the Cuddapah basin. Precamb. Res., 298, 235–251.

Pearce, J.A. (2008). Geochemical fingerprinting of oceanic basalts with applications to ophiolite classification and the search for Archean oceanic crust. Lithos, 100, 14–48.

Rock, N.M.S. (1991). Lamprophyres. Blackie, London, 225p.

Smith, E.I.; Sánchez, A.; Walker, J.D.; and Wang, K. (1999). Geochemistry of mafic magmas in the hurricane volcanic field, Utah: implications for small- and large-scale chemical variability of the lithospheric mantle. J. Geol., 107, 433–448.

Sun, C.M.; and Bertrad, J. (1991). Geochemistry of clinopyroxenes in plutonic and volcanic sequences from the Yanbian Proterozoic ophiolites (Sichuan Province, China): petrogenetic and geotectonic implications. Schweiz. Mineral. Petrog. Mitt., 71, 243–259.

Sun, S.S.; and McDonough, W.F. (1989). Chemical and isotopic systematics of oceanic basalts: implications for mantle composition and processes. In: Saunders, A.D.; Norry, M.J. (Eds.), Magmatism in Ocean Basins. Geol. Soc., London, Spec. Publ., 42, 313–345.

Subrahmanyam, K.; Mallikharjuna Rao, J.; and Leelanandam, C. (1987). Occurrence of lamprophyre dykes near Khammam, Andhra Pradesh. Indian Jour. Geol., 59, 65-70.

Thirlwall, M.F.; Smith, T.E.; Graham, A.M.; Theodorou, N.; Hollings, P.; Davidson, J.P.; and Arculus, R.J. (1994). High field strength element anomalies in arc lavas: source or process? J. Petrol., 35, 819–838.

Thorpe, R.S. (1987). Permian K-rich volcanic rocks of Devon: petrogenesis, tectonic setting and geological significance. Trans. R. Soc. Edinburgh, 77, 361–366.

Turner, S.; Arnaud, N.; Liu, J.; Rogers, N.; Hawkesworth, C.; Harris, N.; Kelley, S.; Van Calsteren, P.; and Deng, W. (1996). Post-collision, shoshonitic volcanism on the Tibetan plateau: implications for convective thinning of the lithosphere and the source of ocean island basalts. J. Petrol., 37, 45–71.

Ulrych, J.; Pivec, E.; Zak, K.; Bendl, J.; and Bosak, P. (1993). Alkaline and ultramafic carbonate lamprophyres in Central Bohemian Carboniferous basins, Czech Republic. Miner. Petrol., 48, 65–81.

Verma, S.P.; and Gómez, M.A. (2013). Computer programs for the classification and nomenclature of igneous rock. Episodes, 36, 115–124.

Wilson, M. (1989). Igneous Petrogenesis: A Global Tectonic Approach. Unwin Hyman, London, 466p.

Wyman, D.A.; and Kerrich, R. (1989). Archean lamprophyre dikes of the Superior province, Canada: distribution, petrology, and geochemical characteristics. J. Geophys. Res., 94, 4667–4696.